Analysis of Integration Gain in Passive Radar

Mateusz Malanowski[#1], Krzysztof Kulpa[#2]

[#]*Institute of Electronic Systems, Warsaw University of Technology*
Nowowiejska 15/19, 00-665 Warsaw, Poland

[1]m.malanowski@elka.pw.edu.pl

[2]kulpa@ise.pw.edu.pl

***Abstract*— This paper investigates various factors influencing the processing gain obtained thanks to coherent integration in a Passive Coherent Location (PCL) radar. In theory, a longer integration time should lead to higher integration gain. In practice, however, some limitations exist, which restrict the maximum attainable processing gain. The paper presents theoretical considerations accompanied by numerical results based on simulated data as well as data acquired with an FM-based PCL system.**

I. Introduction

The continuous wave radar provides high integration gain thanks to the fact that the signal energy is emitted continuously. A special type of continuous wave radar is a passive radar known as PCL (Passive Coherent Location) or PBR (Passive Bistatic Radar). A PCL utilizes illuminators of opportunity, such as radio or television transmitters, in order to detect and track targets.

Because the parameters of the transmitters are not under control of radar system designers, it is necessary to exploit the existing situation as much as possible. Usually, the main desire is to increase the coverage of the system. This can be achieved by increasing the signal to noise ratio (*SNR*). Because the power and bandwidth of the signal are out of the designer's control, the possibilities of influencing the *SNR* are limited. Some of the solutions include increasing the antenna gain or lengthening the integration time. In this paper, the authors are focusing on increasing the integration time.

The purpose of this paper is to investigate the limiting factors of the integration time and present methods allowing to combat some of them. The paper shows simulation results as well as results of processing real-life data acquired with the PaRaDe FM-based system [1]-[3].

II. Integration Gain

The PCL processing is based on correlation of the reference and echo signal. Typically the correlation function has the following form:

$$\psi(R,V)=\int_{-T/2}^{T/2} x_e(t)x_r^*\left(t-\frac{R}{c}\right)\exp\left(-j\frac{2\pi}{\lambda}Vt\right)dt, \quad (1)$$

where $x_e(t)$ is the echo signal, $x_r(t)$ is the reference signal, R is the bistatic range, V is the bistatic velocity, λ is the wavelength, c is the speed of light and T is the integration time.

The correlation process can be considered as coherent integration. Therefore, the signal to noise ratio after correlation can be expressed as:

$$SNR = SNR_{in}BT, \quad (2)$$

where B is the signal bandwidth and SNR_{in} is the input signal to noise ratio. The SNR_{in} can be calculated from the bistatic radar equation [4]. The integration gain (ratio of the SNR and SNR_{in}) is the time-bandwidth product:

$$G = BT. \quad (3)$$

Equations (1) and (2) were derived under the following assumptions:

- Target has constant bistatic velocity
- Signal envelope stretch is negligible
- Target complex amplitude is constant (not fluctuating target)

In reality, these conditions are not always satisfied. In the following sections the violation of each of the assumptions will be discussed.

A. Constant bistatic velocity

Correlation defined by (1) assumes the following target bistatic motion model:

$$r(t)=R+Vt. \quad (4)$$

If the target is characterized by a more complicated motion, a phase mismatch in (1) will arise. Let us assume that the target has a non-zero bistatic acceleration A, therefore the extended motion model can be expressed as:

$$r^*(t)=R+Vt+\frac{At^2}{2}. \quad (5)$$

The phase mismatch between the actual and assumed range models can be calculated from:

$$\Delta\varphi(t)=\frac{2\pi}{\lambda}\left(r^*(t)-r(t)\right). \quad (6)$$

Assuming that the phase difference should not exceed $\pi/2$ at the ends of a symmetrical observation interval, the maximum observation time for a given acceleration can be calculated as:

$$T_{\max}=\sqrt{2}\sqrt{\frac{\lambda}{A}}. \quad (7)$$

However, one can also use the extended motion model of (5) in the correlation function in order to compensate for the

target acceleration. In such a case, an additional quadratic phase component has to be taken into account [5],[6]:

$$\psi(R,V,A)=\int_{-T/2}^{T/2} x_e(t)x_r^*\left(t-\frac{R}{c}\right)\cdot \cdot\exp\left[-j\frac{2\pi}{\lambda}\left(Vt+\frac{At^2}{2}\right)\right]dt \quad (8)$$

The same scheme can be extended for higher order motion components, i.e. jerk (derivative of acceleration), etc.

B. Envelope Stretch

When a signal reflected from a moving target is received, the frequency of the signal is shifted due to the well known Doppler effect. This is also accompanied by a change in the time scale of the received signal. This effect, known as the signal envelope stretch, is usually neglected since the observation time is relatively short. The influence of the envelope stretch can be investigated considering displacement of a target during the observation time relative to the resolution cell. If the displacement is much smaller than the resolution cell, the effect can be ignored. This is usually the case in most pulsed radars. However, in continuous wave radars, when long integration times are employed, the envelope stretch can play a significant role.

If the signal envelope stretch is a source of a mismatch between correlated signals, a modified version of the correlation function should be used [7],[8]:

$$\psi(R,V)=\int_{-T/2}^{T/2} x_e(t)x_r^*\left[t-\frac{r(t)}{c}\right]\cdot \cdot\exp\left[-j\frac{2\pi}{\lambda}r(t)\right]dt, \quad (9)$$

where $r(t)$ is the assumed target motion model. In (9) the reference signal $x_r(t)$ is not only delayed as in (1), but also stretched due to time dependent distance $r(t)$.

In practical realizations, the correlation defined by (1) or (9) is calculated digitally. It means that both the reference and echo signals are sampled before processing. This poses a problem when (9) has to be calculated since the values of the reference signal between sampling instants are required. This can be solved by using resampling methods, described and compared in [7],[8].

C. Target Fluctuations

Target fluctuations are caused by two main factors: a change in the observation angle and the multipath effect. Those two situations will be considered using simple models, which can give rough approximations of fluctuations impact.

First, the change in the observation angle will be investigated in the following scenarios: straight path motion and coordinated turn.

A target can be thought of as an antenna. The width of the main lobe of the antenna pattern can be expressed as:

$$\alpha=\frac{\lambda}{L}, \quad (10)$$

where L is the target length. The angle α can be regarded as the maximum allowable change in the aspect angle.

In the first scenario, the target is moving along a straight path with velocity V_x, perpendicular to the line of sight, as in Fig. 1. The time needed for the aspect angle to change by α can be calculated by:

$$T_{fluct1}\approx\frac{\lambda y_0}{LV_x}, \quad (11)$$

where y_0 is the range to the target. T_{fluct1} can be regarded as the maximum integration time, which does not introduce significant losses in processing gain.

In the second scenario, the target is following a circular trajectory with velocity V_t and centrifugal acceleration A_c (Fig. 2). The angular velocity can be expressed as:

$$\omega=\frac{A_c}{V_t}. \quad (12)$$

The change of the target angle over time is the product of the angular velocity and time. By limiting the change to the width of the main lobe of the target radiation pattern α, the following equation can be obtained:

$$T_{fluct2}=\frac{\lambda V_t}{LA_c}. \quad (13)$$

The second of the main sources of fluctuations is the multipath effect. The signal impinging on the target or radar is usually the sum of the direct component and multipath components. Those two kinds of contributions interfere with each other causing target fluctuations.

A simplistic model of the multipath effect with a single reflection and a flat earth model is shown in Fig. 3. The heights of the radar and the target are h_1 and h_2, respectively. The incidence and reflection angles are equal and denoted as β. The length of the direct path is equal to:

$$R_d=\sqrt{(h_1-h_2)^2+(x_1+x_2)^2}=\sqrt{(h_1-h_2)^2+x_0^2}. \quad (14)$$

The length of the reflected path is equal to:

$$R_r=R_{r1}+R_{r2}=\sqrt{h_1^2+x_1^2}+\sqrt{h_2^2+x_2^2}, \quad (15)$$

where, using basic geometric relations, $x_1=x_0h_1/(h_1+h_2)$ and $x_2=x_0h_2/(h_1+h_2)$. The distance between the target and the radar x_0 is the sum of distances x_1 and x_2. It depends on time since the target is moving with velocity V_x.

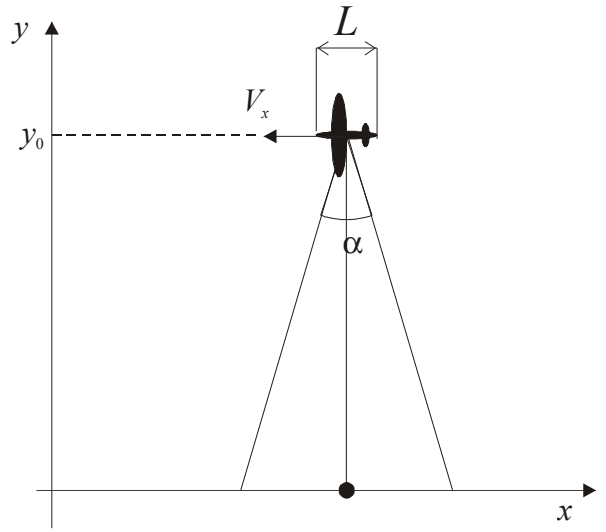

Fig. 1 Geometry for calculation of change in the observation angle due to straight line motion

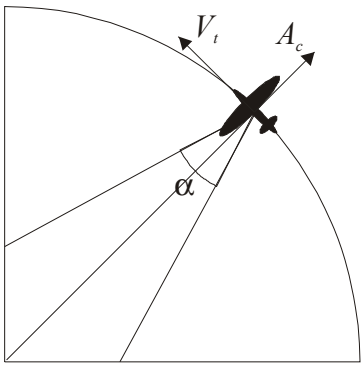

Fig. 2 Geometry for calculation of change in the observation angle due to target turn

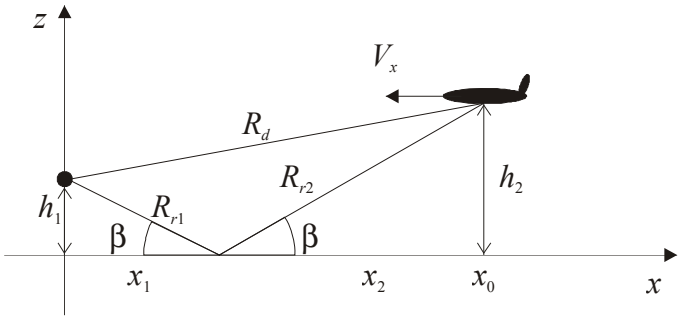

Fig. 3 Geometry for calculation of fluctuation time caused by multipath effect

The phase difference between direct and reflected components can be calculated from:

$$\Delta\varphi(t)=\frac{2\pi}{\lambda}(R_d-R_r), \tag{16}$$

and it is time dependent. The fluctuation time can be defined as the time needed for phase difference to change by a certain value, e.g. $\pi/2$:

$$\Delta\varphi(T_{fluct3})=\frac{\pi}{2}. \tag{17}$$

The integration time should not exceed the fluctuation time, therefore, the fluctuation time T_{fluct3} sets a limit for the integration time. Due to the presence of the square roots in (14) and (15), calculation of the fluctuation time requires solving a nonlinear equation.

The presented calculations assume a flat earth model. For further ranges, a spherical earth model might be required, which will lead to more elaborate equations. However, simple approximations can be employed, namely for a small height of the radar the same equations can be used after applying correction to the height of the target equal to $-x_0/(2R_e)$, where R_e is the radius of the earth.

The presented methods for calculating fluctuation times assume very simple models, which may not be very accurate compared with real scenarios. Since PCL is characterized by the bistatic geometry, the situation is all the more complicated. However, even those calculations should provide useful information concerning the expected orders of fluctuation times.

III. Numerical Results

A. Simulations

In order to verify the analytical consideration presented so far, the authors have carried out a series of experiments on simulated data. All experiments were conducted assuming parameters typical for an FM-based PCL: B = 50 kHz, λ = 3 m. The reference signal was simulated as complex Gaussian noise, with given bandwidth B. The target signal in the echo channel was simulated as a delayed and Doppler-shifted copy of the reference signal. In the appropriate simulations, the acceleration and envelope stretch were also added. The output signal to noise ratio was measured as the ratio of the peak of the correlation function to the mean noise floor level. Based on [9] and [10] it can be shown that when the noise floor results from the received noise and not the waveform sidelobes, the peak-to-noise-floor ratio is equivalent to the *SNR*.

The parameters of the simulations were chosen so that the output *SNR* is in the range of 25-45 dB. Such high values of *SNR* were set on purpose in order to minimize the error of the peak value measurement caused by random noise fluctuations. The presented curves, however, have the same character for weaker echoes, which are the main focus of the presented procedures.

First, the influence of an inappropriate motion model was investigated. Fig. 4 shows the *SNR* versus integration time for different values of acceleration. The envelope stretch was neglected in this experiment. Since the correlation was calculated according to (1), the acceleration was not taken into consideration. It can be seen that higher values of acceleration

cause integration gain to drop from the theoretical value for shorter integration times. The maximum integration times calculated according to (6) are: 7.75, 2.45 and 0.77 s for accelerations 0.1, 1, and 10 m/s^2 respectively. These values are marked on the plot by vertical lines and show good correspondence with the curves obtained.

Fig. 5 shows the impact of the signal envelope stretch on the *SNR*. In the experiment, the target motion model consisted of two components: bistatic range and velocity. Higher bistatic velocities result in greater losses if the envelope stretch is not compensated. For typical parameter values of FM-based PCL, the significant losses are introduced only for high velocities (over 1000 m/s) and long integration times. For this reasons, the envelope stretch in FM PCL can be neglected in most of the cases. When other types of transmitters are exploited, e.g. DAB or DVB-T, the change of the time scale will affect the processing to a greater extent.

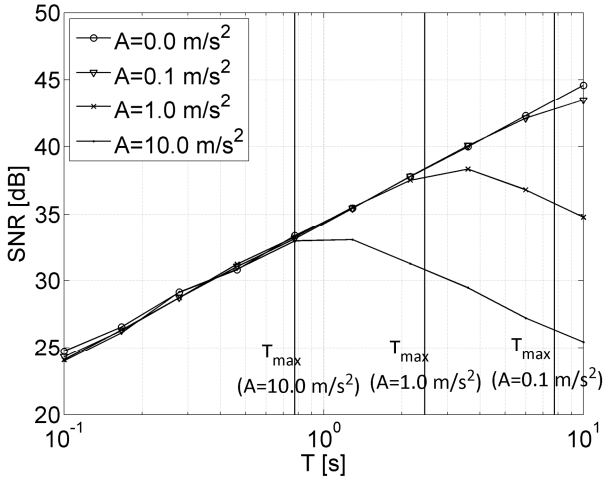

Fig. 4 *SNR* versus integration time for different values of acceleration

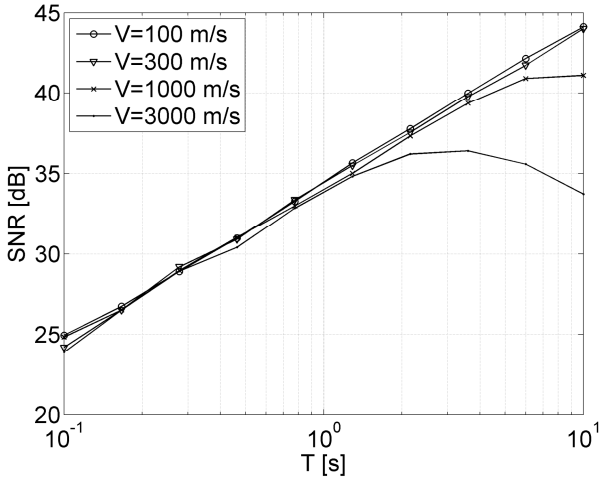

Fig. 5 *SNR* versus integration time without envelope stretch compensation

The curves of fluctuation time due to the change in the observation angle caused by a straight line motion, calculated using equation (11), are depicted in Fig. 6. The velocity of the aircraft was set to V_y=300m/s. The three curves correspond to three different sizes of aircraft: 15m (jet fighter), 40m (medium size jet liner) and 70m (Jumbo jet). It can be seen that shorter ranges result in shorter fluctuation times due to a smaller cross-section of the main lobe of the pattern. Larger targets are characterized by shorter fluctuation time because of the narrower main lobe of the pattern.

In Fig. 7 one can observe fluctuation times caused by the target turning for three sizes of the target. The velocity of the aircraft was equal to V_t=300m/s. The typical values of centrifugal acceleration are 10m/s^2 (app. 1g) for a jet liner and up to 50m/s^2 (app. 5g) for a jet fighter. Higher centrifugal acceleration corresponds to a smaller radius of the turn. The fluctuation time is of the order of tens of seconds for lazy turns. However, faster turns (smaller radius) cause the fluctuation time to drop rapidly. The effect is more visible in the case of larger targets, where the main lobe width is smaller.

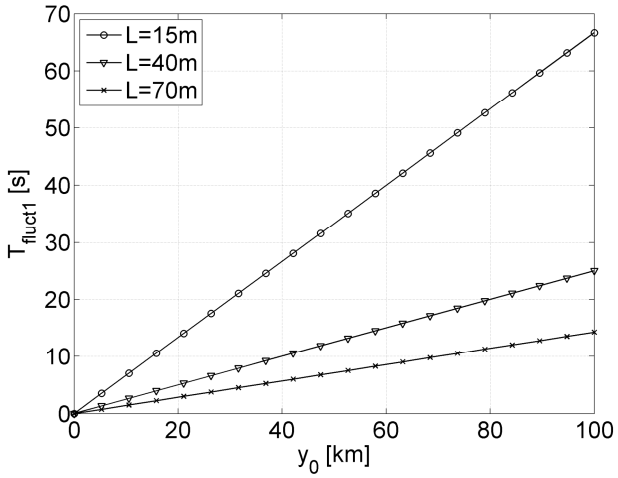

Fig. 6 Fluctuation time due to the change of the observation angle \caused by straight line motion

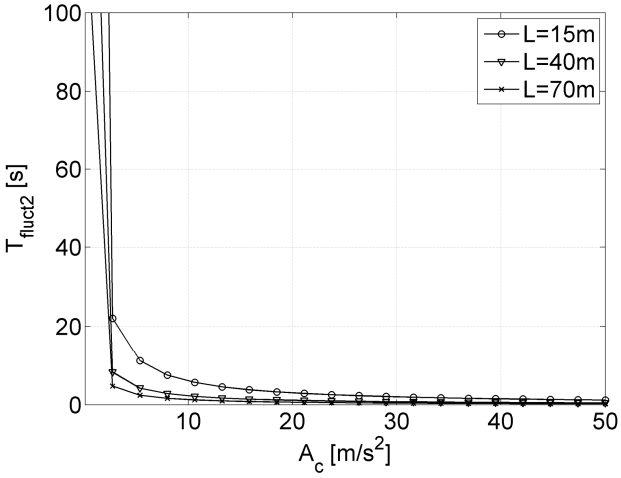

Fig. 7 Fluctuation time due to the change of the observation angle caused by turning target

Fig. 8 shows fluctuation times caused by the multipath effect. The following values were used: target velocity V_x = 300m/s and radar antenna height h_1 = 50m. Different

curves correspond to different target altitudes h_2 = 100, 1000, 1000m. For low flying targets, the fluctuation time increases rapidly with range. For high flying targets, the values of the fluctuation times are lower and increase steadily with the range to the target.

The presented experiments show that the fluctuation time increases with range. For far targets, with a range larger than 80km, the fluctuation time is longer than 10s. In such cases, a long integration time can be used. For near targets, the fluctuation time can be shorter than 1s, but usually the *SNR* for such targets is significantly higher and there is no need for applying a long integration time.

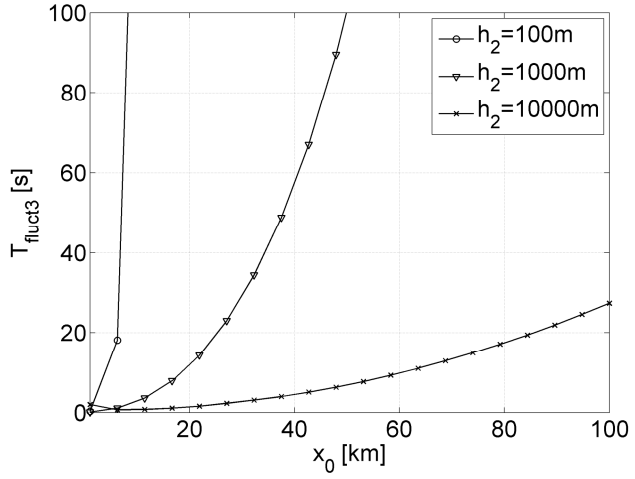

Fig. 8 Fluctuation time due to the multipath effect

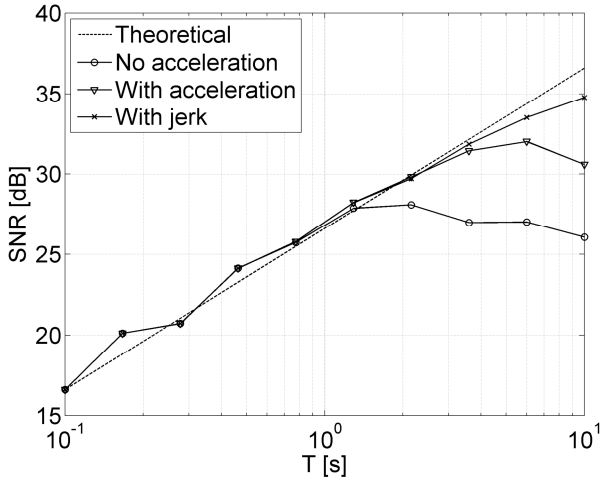

Fig. 9 *SNR* for a real target echo for different versions of correlation function

B. Real-life data

The data used in this part of the paper were recorded with the PaRaDe (Passive Radar Demonstrator) system developed at Warsaw University of Technology [1]-[3]. The target chosen for this experiment is an aircraft at $R \approx 20$km, $V \approx$ -150m/s (bistatic values). Due to the close range, the target motion causes rapid changes in the bistatic geometry, therefore the bistatic parameters vary with time significantly.

Fig. 9 shows *SNR* curves for different versions of the correlation function for the selected target echo. The curve representing the theoretical value of the *SNR* was calculated as a linear extrapolation of the measured *SNR* for short integration times. When the basic correlation procedure (1) is used, the measured *SNR* starts to differ from the theoretical one for the integration time equal to 1.3s. In the correlation process as in (8), if the extended target model is used, one obtains a plot following the theoretical one up to 3.6s. The acceleration for the extended target model was calculated using methods described in [6]. For a longer integration time, the acceleration compensation is not satisfactory. Introducing jerk (i.e. derivative of acceleration) into the correlation procedure results in further improvement of *SNR* for long integration times. In the experiment, the jerk was calculated by comparing the acceleration values at different time instants. It can be seen that the *SNR* value for 10 s is close to the theoretical one when the extended motion model is used.

Measuring the signal bandwidth, one can calculate the input *SNR* and the integration gain. In the example under consideration, the signal bandwidth was approximately 50kHz. Therefore, for 10s integration time, the input *SNR* is – 22dB and the integration gain is 57dB.

IV. Conclusions

The paper summarizes the factors limiting processing gain obtained in coherent correlation process in a PCL radar. Some of the limitations can be alleviated by extending the target motion model or by introducing the stretch of time scale of the reference signal. Other factors, such as fluctuations, are more difficult to combat, but simple calculations enable us to predict the values of the fluctuation times and define maximum integration times.

In order to extend the correlation time to higher values, it might be necessary to incorporate acceleration and jerk to correlation processing. For extremely fast targets it is also necessary to apply stretch processing. The experiments with recorded signals showed that for a typical FM-based PCL integration time up to 10 s can be used after application of the extended target motion model.

The increase of the correlation time is important primarily for weak echoes, which originate from small or distant targets. The authors showed that the expected fluctuation time increases with the range to the target. For this reason, the distant targets can be detected by applying long integration times. The close targets, which may have short fluctuation times, usually have high *SNR* and a long integration time is not required.

It is worth noting that increasing the *SNR* is not always the priority. In [11] authors investigated the relationship between the integration time and the average track confirmation time. It was shown that there is an optimum value of the integration time which provides the minimum track confirmation time for a given input *SNR*. For this reason, the processing gain should be analyzed in the context of the whole system in order to obtain the best results. This paper provides a useful

framework which can be incorporated into a joint analysis of a passive radar system.

ACKNOWLEDGMENT

This work was supported by the Polish Ministry of Science and Higher Education under Commissioned Research Project PBZ-MNiSW-DBO-04/I/2007.

REFERENCES

[1] K. Kulpa, and M. Malanowski, "Simple COTS PCL Demonstrator," in *Proc. 5th Multi-National Passive Covert Radar Conference*, 13-15 November 2007, Shrivenham, UK, on CD.

[2] M. Malanowski, G. Mazurek, K. Kulpa, and J. Misiurewicz, "FM based PCL radar demonstrator," in *Proc. International Radar Symposium 2007*, 5-7 September 2007, Cologne, Germany, pp. 431-435.

[3] M. Malanowski, K. Kulpa, J. Misurewicz, "PaRaDe – Passive Radar Demonstrator Family Development at Warsaw University of Technology," in *Proc. Microwaves, Radar and Remote Sensing 2008*, Kiev, Ukraine, 22-24 September 2008, (to be published).

[4] H.D. Griffiths, and C.J. Baker, "Passive coherent location radar systems. Part 1: Performance prediction," *IEE Proc.-Radar Sonar Navig*., Vol. 152, No. 3, June 2005.

[5] K. Kulpa, "Target Acceleration Estimation for Continuous Wave Noise Radar," in *Proc. of International Radar Symposium 2005*, 06-08 September 2005, Berlin, Germany, pp. 177–183.

[6] M. Malanowski, and K. Kulpa, "Acceleration estimation for Passive Coherent Location radar," in Proc*. of RadarCon 2008*, 26-30 May 2008, Rome, Italy, pp. CD.

[7] K. Kulpa, and J. Misiurewicz, "Stretch Processing for Long Integration Time Passive Covert Radar," In *Proc. International Conference on Radar 2006*, Shanghai, China, 16-19 October 2006, pp. 496-499.

[8] J. Misiurewicz, K. Kulpa, "Compensation of envelope stretch in long integration time noise radars," in *Proc. International Radar Symposium 2007*, 05-07 September 2007, Cologne, Germany, pp. 89-93.

[9] S.R.J. Axelsson, "Noise radar for range/Doppler processing and digital beamforming using low-bit ADC," *IEEE. Trans. Geoscience and remote sensing,* vol. 41, no. 12, December 2003, pp. 2703-2720.

[10] S.R.J. Axelsson, "Noise radar for using random phase and frequency modulation," *IEEE. Trans. Geoscience and remote sensing,* vol. 42, no. 11, November 2004, pp. 2370-2384.

[11] M. Malanowski, "Influence of Integration Time on Tracking Performance in PCL Radar," in *Proc. of Photonics Applications in Astronomy, Communications, Industry, and High-Energy Physics Experiments 2007* (Proceedings Volume), vol. 6937.